

Environmental Research Letters



LETTER

Understanding spatial variability of methane fluxes in Arctic wetlands through footprint modelling

OPEN ACCESS

RECEIVED

15 December 2018

REVISED

10 October 2019

ACCEPTED FOR PUBLICATION

11 October 2019


PUBLISHED

16 December 2019

Original content from this work may be used under the terms of the [Creative Commons Attribution 3.0 licence](#).

Any further distribution of this work must maintain attribution to the author(s) and the title of the work, journal citation and DOI.



Kassandra Reuss-Schmidt^{1,2,3,7} , Peter Levy³, Walter Oechel^{2,6}, Craig Tweedie⁴, Cathy Wilson⁵ and Donatella Zona^{1,2,7}

¹ Department of Animal and Plant Sciences, University of Sheffield, Western Bank, Sheffield, S10 2TN, United Kingdom

² Global Change Research Group, Dept. Biology, San Diego State University, San Diego, CA 92182, United States of America

³ Centre for Ecology and Hydrology Bush Estate, EH10 Edinburgh, United Kingdom

⁴ Department of Biological Sciences, University of Texas at El Paso, TX 79968, United States of America

⁵ Los Alamos National Lab, PO Box 1663 Los Alamos, NM 87545, United States of America

⁶ Department of Geography, University of Exeter, Exeter, EX4 4RJ, United Kingdom

⁷ Authors to whom any correspondence should be addressed.

E-mail: schmidt1@sheffield.ac.uk and d.zona@sheffield.ac.uk

Keywords: eddy covariance, footprint modelling, heterogeneity, permafrost, wetlands, Arctic, ecosystem feedbacks

Supplementary material for this article is available [online](#)

Abstract

The Arctic is warming at twice the rate of the global mean. This warming could further stimulate methane (CH₄) emissions from northern wetlands and enhance the greenhouse impact of this region. Arctic wetlands are extremely heterogeneous in terms of geochemistry, vegetation, microtopography, and hydrology, and therefore CH₄ fluxes can differ dramatically within the metre scale. Eddy covariance (EC) is one of the most useful methods for estimating CH₄ fluxes in remote areas over long periods of time. However, when the areas sampled by these EC towers (i.e. tower footprints) are by definition very heterogeneous, due to encompassing a variety of environmental conditions and vegetation types, modelling environmental controls of CH₄ emissions becomes even more challenging, confounding efforts to reduce uncertainty in baseline CH₄ emissions from these landscapes. In this study, we evaluated the effect of footprint variability on CH₄ fluxes from two EC towers located in wetlands on the North Slope of Alaska. The local domain of each of these sites contains well developed polygonal tundra as well as a drained thermokarst lake basin. We found that the spatiotemporal variability of the footprint, has a significant influence on the observed CH₄ fluxes, contributing between 3% and 33% of the variance, depending on site, time period, and modelling method. Multiple indices were used to define spatial heterogeneity, and their explanatory power varied depending on site and season. Overall, the normalised difference water index had the most consistent explanatory power on CH₄ fluxes, though generally only when used in concert with at least one other spatial index. The spatial bias (defined here as the difference between the mean for the 0.36 km² domain around the tower and the footprint-weighted mean) was between |51|% and |18|% depending on the index. This study highlights the need for footprint modelling to infer the representativeness of the carbon fluxes measured by EC towers in these highly heterogeneous tundra ecosystems, and the need to evaluate spatial variability when upscaling EC site-level data to a larger domain.

1. Introduction

Methane (CH₄) emissions from Arctic permafrost soils are a major source of uncertainty in the region's future global warming potential (Schuur and Abbott 2011, IPCC 2013). The Arctic is warming at twice the rate of the global mean (Blunden and Arndt 2019) and its frozen

permafrost soils store 1300–1370 Pg of organic carbon (Hugelius *et al* 2014), twice the current atmospheric stock (IPCC 2013). By the year 2300, thawing permafrost could release between 381 and 616 Pg of carbon to the atmosphere (Schuur *et al* 2013); and it is imperative to know how much of this carbon will be released as CH₄, which on a per-molecule basis has a global warming

potential 25–28 times greater than carbon dioxide (CO₂) (Forster *et al* 2007, Etminan *et al* 2016). One method of measuring trace gas fluxes central to understanding the current and future carbon budget is the eddy covariance (EC) technique, as it can bridge the gap between smaller plot scale chamber measurements and larger regional scale remotely sensed (RS) data from aircraft and satellite (Baldocchi 2003, Chen *et al* 2009). There are, however, challenges to using this technique in the Arctic's heterogeneous landscapes (Davidson *et al* 2016) as it assumes a uniform sampling area (Foken and Wichura 1996). One approach used to address this issue is footprint modelling (Vesala *et al* 2008).

The spatial heterogeneity of Arctic wetlands is often related to the presence of cryogenic processes, where the formation and degradation of ice wedges, leads to patterned ground formations such as polygonal tundra (Brown 1967). The polygons consist of distinct microtopographic features, namely rims, troughs and polygon centres, which each have distinct CH₄ emission rates (Sachs *et al* 2010, Lara *et al* 2015, Davidson *et al* 2016, Vaughn *et al* 2016). These features have differential water drainage and soil moisture, a well-established driver of CH₄ production and consumption, with water-logged anaerobic areas producing CH₄ and dry areas sometimes acting as slight CH₄ sinks (Valentine *et al* 1994, Segers 1998, Sachs *et al* 2010, Von Fischer *et al* 2010, Lipson *et al* 2012). Typically, rims are well-drained, while troughs are inundated, with polygon centres being either convex (high-centres) or concave (low-centres), depending on age, and thus dry or wet respectively. Microtopography also influences plant (Joabsson *et al* 1999, Von Fischer *et al* 2010) and even microbe (Taş *et al* 2018) distributions which likewise impact CH₄ production and efflux. Sedges grow in water logged areas and release organic acid root exudate that increases CH₄ production, furthermore, a number of species have aerenchymal tissue which allows CH₄ to avoid oxidation by passing through the plant (McEwing *et al* 2015, Andresen *et al* 2017). Additionally, Arctic wetlands are further mosaiced due to the thermokarst thaw lake cycle (Zona *et al* 2009, Sturtevant and Oechel 2013). These lakes periodically drain, leaving depressions and drainage channels that vary in the same factors affecting CH₄ emission in polygonal tundra. In addition to spatial variation, CH₄ fluxes vary over time, as water table, thaw depth, soil temperature, plant productivity, and the available carbon pool, all major controls on CH₄ production, change throughout the year (Zona *et al* 2009, Lipson *et al* 2012, Zheng *et al* 2018).

A flux tower footprint defines the area being sampled by the EC tower (Leclerc and Thurtell 1990, Horst and Weil 1994). Footprint modelling has been used to enable the interpretation of EC data in variable landscapes (Schmid and Lloyd 1999, Göckede *et al* 2006, Parmentier *et al* 2011, Tuovinen *et al* 2018), by assigning relative flux contribution to specific areas based on tower height, wind speed and direction, and

turbulence (Leclerc and Thurtell 1990, Schuepp *et al* 1990, Burba and Anderson 2010). There are a few different types of footprint models including one- and two-dimensional analytic models, Lagrangian, large eddy simulations, and closure models (Vesala *et al* 2008). Of these, the most commonly used are the analytical models, specifically the Kormann and Meixner (2001), Kljun *et al* (2004), and Hsieh *et al* (2000) models, due to having relatively low computational complexity and their applicability in a wide array of experiments (Vesala *et al* 2008, Leclerc and Foken 2014).

Footprint modelling has been utilised in several ways to interpret flux variability in the Arctic. One way footprint modelling can be used is to relate EC measurements to chamber measurements by upscaling them to the EC footprint. In a sub-Arctic mire site in Finland, the Kormann and Meixner (2001) footprint model was applied to get half-hourly footprint-weighted spatial indices, these were used as input for a process-based model and improved the correlation between growing season upscaled chamber CH₄ fluxes and EC flux estimates, with an increase in r^2 from 0.41 to 0.72 (Hartley *et al* 2015). Budishchev *et al* (2014) also used a footprint model to upscale the chamber measurements to the EC scale, improving the r^2 correlation coefficient from 0.14 to 0.7, in a Russian polygonal tundra. Davidson *et al* (2017) show a 20%–30% improvement and an r^2 of 0.88, across several tundra sites in Alaska by using footprint modelling to upscale chamber measurements to the EC tower fluxes. One can also use footprint modelling when upscaling fluxes to estimate sensor location bias (Schmid and Lloyd 1999). This metric is the percent difference of a spatial variable's mean within the footprint and the mean of the user-defined area to which one is upscaling. In a study across the entire Canadian flux network (Chen *et al* 2011), sensor bias was assessed through the distribution of enhanced vegetation index and normalised difference vegetation index (NDVI) showing that four out of twelve sites presented a difference higher than 5% between the EC tower annual footprints (with 90% of the footprint generally within a 1 km² radius) and the surrounding area (measured at 1, 2, and 3 km² centred at the tower base). Importantly the sites with the highest bias, ranging from –14% to 9%, were classified as ombrotrophic bog (Chen *et al* 2011), a vegetation type similar to sites evaluated in this study. More recently, in Siberian tundra Tuovinen *et al* (2018) used footprint modelling on a half-hourly time scale to parse CH₄ sources and sinks by vegetation type, they also looked at the sites sensor location bias and found a 14% when looking at leaf area index regarding the wider 6.3 km² around the base of the tower.

The aim of this study is to evaluate the effect of spatial heterogeneity on the CH₄ fluxes measured by EC method at two tundra sites located on a large wetland area in the North Slope of Alaska. First, we

assessed whether the area sampled by the EC measurement, as characterised by the footprint, was representative of the 0.36 km² domain around the tower. This was done to determine if the area around the base of the tower was suitable to link to RS data for the purpose of upscaling. We then used statistical modelling, to separate the variability in the measured flux arising from the (i) temporal variability in the environmental controls on the CH₄ fluxes (temperature, soil moisture etc), and (ii) the variability in the footprint, which sampled different parts of the surrounding landscape at different times. We expect the spatial variability in the landscape to have a substantial influence on the fluxes. We also expect that there may be significant sensor bias between the tower footprint and the domain around the tower, due to the inherent heterogeneity of polygonal tundra, which would need to be considered for upscaling the fluxes.

2. Methods

2.1. Study sites

Two EC towers located near Barrow (Utqiagvik), on the North Slope of Alaska, were used in this study (figure 1). Average annual temperature and precipitation measured at the Barrow weather station, between 1948 and 2013, were −11.3 °C and 72 mm respectively (Zona *et al* 2016). The two tower sites utilised for this study include the and Biocomplexity Experiment South (BES) and barrow environmental observatory (BEO). BES and BEO are less than 1 km apart and have similar environmental conditions. The sites share similar vegetation cover, namely sedges (*Eriophorum russeolum*, *Carex aquatilis*), grasses (*Poa arctica*), and mosses (*Dicranum spp.*) with heights well below 40 cm (Davidson *et al* 2016). A portion of the footprint area for each of these sites takes the form of well-developed polygonal tundra. Additionally, a substantial part of the footprint in BES is occupied by a drained lake basin (figures 1, 2). The water table within these sites is highly variable given the very different microtopography. Polygon rims are well-drained, while the polygon centres and the drained lake areas have high variability in water table (~20 cm seasonal range), with some troughs and particularly low-lying areas remaining inundated through most of the summer (Zona *et al* 2009).

2.2. EC measurements and footprint modelling

EC data were collected at 10 Hz with a Campbell Scientific CSAT-3 sonic anemometer and a closed-path LGR analysers (FGGA, Los Gatos Research, Mountain View, CA, USA) at a height of ~2–3 m (BES: 2.20 m, BEO: 3.12 m). Fluxes were calculated with the EddyPro software package (LI-COR) based on the methodology described in Zona *et al* (2016). Data were filtered to remove spikes and data unsuitable for footprint modelling as described in Goodrich *et al* (2016) and

Foken *et al* (2004). Measurement of CH₄ at these sites between July of 2013 and November 2015 is used in this study. The EC data used in this study can be accessed via the Arctic Data Centre (Zona 2019).

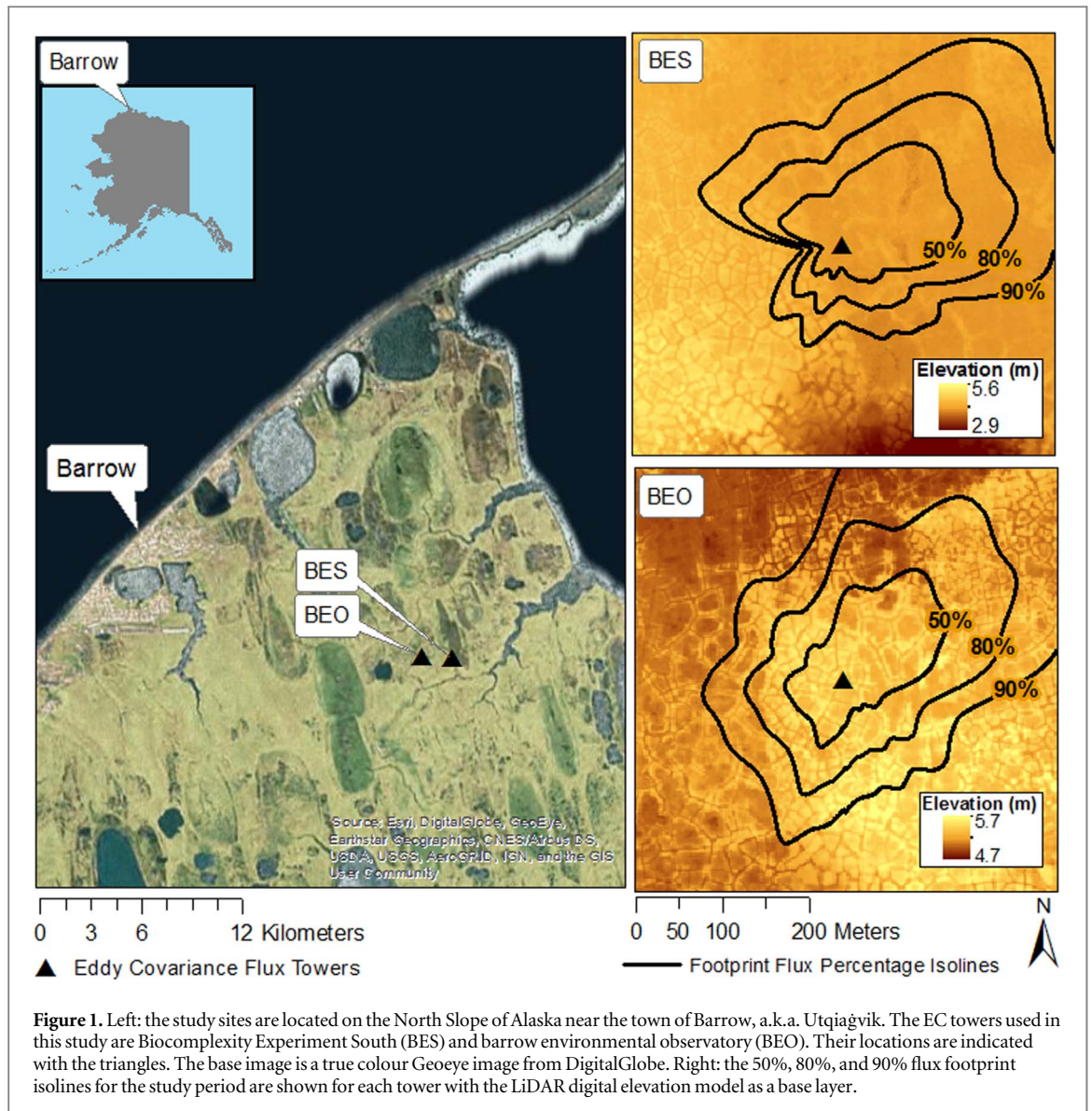
The model of (Kormann and Meixner 2001) was applied on a 600 × 600 m (0.36 km²) grid around the towers to calculate the flux footprint for each half-hourly period (equation (1)). This domain size was chosen based on the assumption that most of the measured fluxes originates within a radius equal to 100 times the height of the tower (Burba and Anderson 2010). During stable atmospheric conditions footprints are elongated and diffuse, leading to some of footprint falling outside of the 0.36 km² around the base of the tower. This was tolerated up to the point where >15% of the footprint was outside the 0.36 km² area, after which footprints were excluded from the analysis. The grid spatial resolution was set to 1 m², so that the small-scale variability of the polygon troughs was represented. With this model, the probability of a grid cell with co-ordinates x, y contributing to the measured flux is:

$$w = \phi(x, y) = \frac{1}{\sqrt{2\pi}\sigma_v x^L} \exp\left(-\frac{y^2}{2(\sigma_v x^L)}\right) u^* x^{-h} \exp\left(-\frac{u(h)}{x}\right), \quad (1)$$

where σ_v is the standard deviation of lateral wind speed, L is the Monin–Obukov length, u^* is the friction velocity, h is the height of the sensor, and $u(h)$ is the horizontal wind velocity at the measurement height. Thus, w represents the relative contribution of each grid cell to the measured flux. The raster grid of each half-hourly footprint, w , can then be used as a weighting factor to calculate the footprint-weighted average of each of the spatial variables, such as elevation or NDVI.

2.3. Temporal and spatial variables

At our towers, several variables used to explain CH₄ variation were collected. Photosynthetically active radiation (PAR) was measured at both sites with the LI-190 LI-COR quantum sensors. A soil temperature (T_s) profile was measured with thermocouples (type-T or type E; Omega Engineering, OMEGA Engineering) at 0, −10, −20 cm at BES and BEO. A soil moisture profile recording soil water content (SWC) was measured at BES with sensors at −10, −20, and −30 cm using Campbell Scientific Water Content Reflectors (CS616). Air temperature (TA) was measured using a Vaisala HMP 45 at the height of the tower at all sites. The Campbell Scientific CSAT-3 sonic anemometer recorded atmospheric stability (Zol), friction velocity (u^*), and air pressure (P_A). In addition, one RS temporal data set was derived from the MODIS satellite 16 d composite max NDVI product (MOD13Q1, Collection-5), which has a resolution of 250 m, and was extracted from the pixel



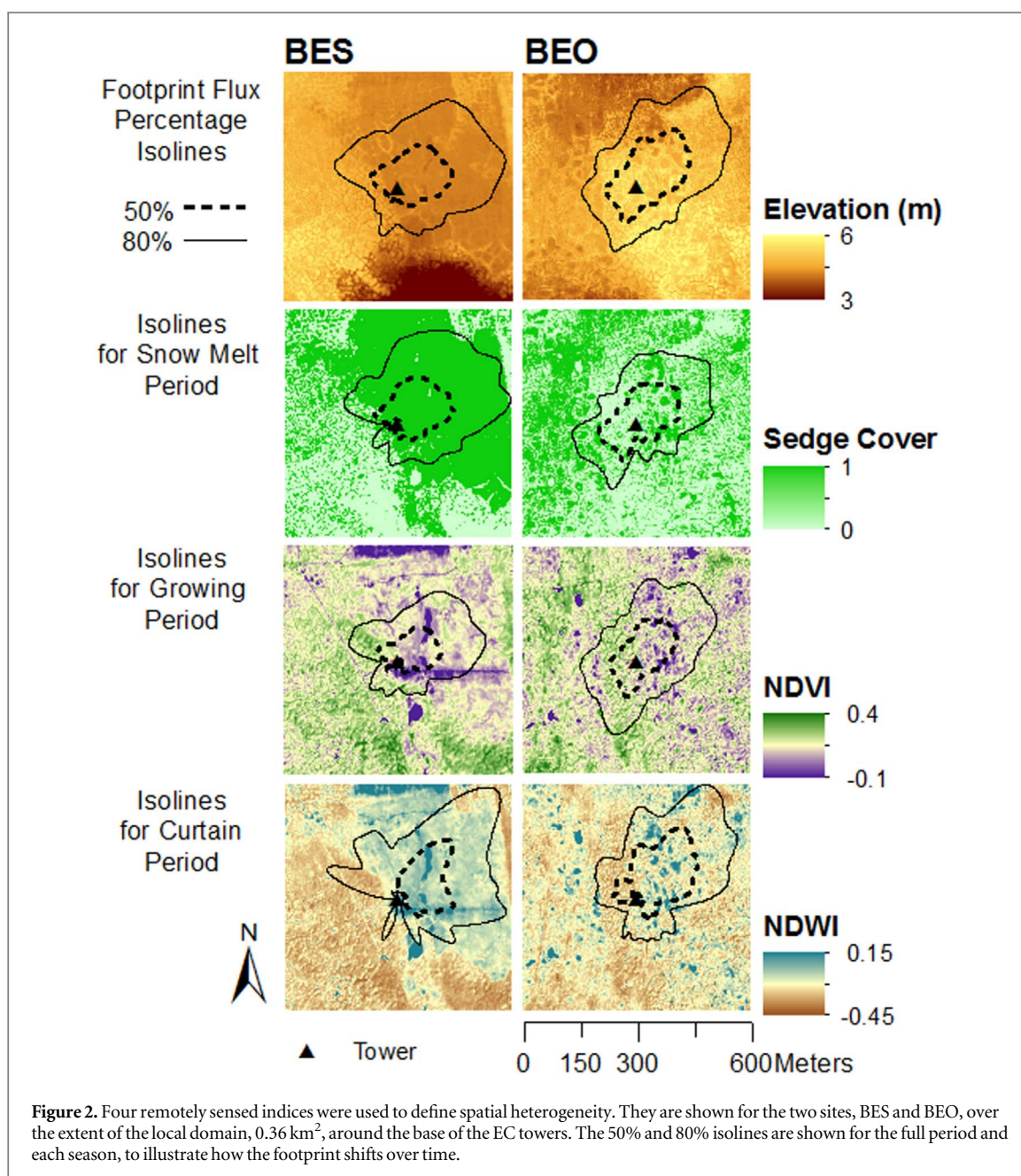
containing BES and the majority of BEO's footprint. It was obtained from the NASA data portal for the duration of the study period (Didan 2015). A LOcally Estimated Scatterplot Smoothing (LOESS) curve was fitted to MODIS data to provide a continuous time series for NDVI

$$\text{NDVI} = \frac{\text{NIR} - R}{\text{NIR} + R} \quad (2)$$

The spatial metrics used in this study were obtained as follows. High resolution topographic data was derived from an airborne LiDAR survey conducted on 12 July 2013 (Wilson and Altmann 2015). The LiDAR derived digital elevation model (DEM) has a horizontal resolution of 0.25 and a 0.143 m vertical resolution. A WorldView-2 (WV2) multispectral satellite image collected on the 6th of July 2013 was used to calculate NDVI and normalised difference water index (NDWI)

$$\text{NDWI} = \frac{G - \text{NIR}}{G + \text{NIR}} \quad (3)$$

This image consists of 8 spectral bands with a 1.84 m horizontal resolution. Only this image was used in this study, as it is the only WV2 image collected during the study period, June 2013 to Dec 2015, free of clouds and snow. Sedge cover was obtained from the wetlands map created by the BAID project (Barrow Area Information Database) (Andresen *et al* 2017), this product is also derived from WV2 data and classifies the Barrow area according to the US Fish and Wildlife Service National Wetlands Inventory Code. For this study, we reclassified the map to presence/absence data for sedge cover, with classes PEM1A–PEM1F indicating sedge cover (where PEM stands for palustrine area with emergent vegetation and the 1A–1F relates to the duration of annual inundation). From these datasets, four indices were calculated to characterise spatial heterogeneity (figure 2). These included elevation (Elev), derived from the LiDAR DEM,



sedge cover, and the NDVI, equation (2) and NDWI, equation (3), (Gao 1996), which are band ratios measuring greenness and wetness respectively calculated from the WV2 image.

For each of the four spatial indices (Elevation, NDWI, NDVI, and Sedge Cover), we weighted the values of the index (\hat{I}_t) on the spatial grid with the footprint probabilities w_t (equation (5)), at each half-hourly time step t of EC data

$$\hat{I}_t = \sum I w_t. \quad (5)$$

This yielded a time series of the spatial indices (\hat{I}), which show the changes in ecosystem properties sampled by the tower footprint as it responded to shifts in wind speed and direction. For the metrics of $\overline{\text{NDVI}}$ and $\overline{\text{NDWI}}$, it should be noted that only a single image

was available, so we assume the values reflect a pattern of spatial variability which stays consistent over time.

The footprint-weighted spatial indices (\hat{I}) were compared with their mean value in the 0.36 km² domain around the base of the tower. This domain was chosen because we aimed to examine whether tower footprints were representative of area from which RS data would typically be extracted, as a general assumption for EC towers is that the majority of flux occurs within a radius of 100 times the height of the tower (Burba and Anderson 2010). Thus, one would normally expect the footprint values and the local domain to be very similar. As a summary statistic, we calculated the sensor location bias (sigma, δ) developed by Schmid and Lloyd (1999) and Chen *et al* (2011)

$$\delta = \frac{\hat{I} - \bar{I}}{\bar{I}}, \quad (6)$$

where \hat{I} is the footprint-weighted spatial index, and \bar{I} is the mean value of that index over the 0.36 km² domain. Therefore, δ characterises the difference between the spatial properties that are sampled by the flux tower and the local mean.

2.4. Statistical analysis

We used linear regression modelling to evaluate the explanatory power of the spatial and temporal variables on CH₄ flux. First, we included all terms (i.e. the temporal variables and the spatial indexes) into a full model of the CH₄ fluxes. The temporal variables used were air temperature (T_A), soil temperature (T_S), SWC, PAR, atmospheric stability (Zol), friction velocity (u^*), air pressure (P_A), and NDVI from the MODIS satellite ($\text{NDVI}_{\text{MODIS}}$). While the spatial variables were $\widehat{\text{Elev}}$, $\widehat{\text{NDVI}}$, $\widehat{\text{NDWI}}$, and $\widehat{\text{Sedge}}$. Model selection used a stepwise regression based on the Akaike information criterion, a widely used goodness of fit criteria. The adjusted R-squared was used to assess the model's explanatory power. To test collinearity in the explanatory variables, the variance inflation factor (VIF) was also calculated and variables that were collinear (VIF > 10) were not included in the same model. The variables retained in the model would thus be significant with regards to influencing CH₄ flux variability. Analysis of variance (ANOVA) was used to ensure that model iterations of the model were statistically different from one another. The same model selection process described here for the full model was applied in all subsequent models. Furthermore, we separated the data by site and season, as well as, modelling CH₄ fluxes, using only either the temporal or spatial variables.

Additionally, to more fully isolate the impact of spatial variability in the footprint (i.e. difference between true temporal variability and spatial variability), a two-step analysis was performed as follows. Firstly, we fitted a linear model of CH₄ flux as function of the temporal variables. This thereby accounted for the temporal variation in the fluxes. We then fitted a model to the residuals of this linear model, including only the footprint-weighted spatial indices to examine whether some of the remaining variation could be accounted for by the spatial heterogeneity.

We also examined seasonal and site influences on flux by including them as factors in the full model. Both season and site were significant in explaining the variability in CH₄ fluxes. Three seasonal periods were defined based on the CH₄ flux rates. The snow melt period began with the first non-zero CH₄ flux measurement of the year and ending when $\text{NDVI}_{\text{MODIS}}$ reached a value of 0.3, which corresponds to a productive grassland (Didan 2015). From that point the growing season period lasted until $\text{NDVI}_{\text{MODIS}}$ again went below 0.3. Then came the post-growing season, which

Table 1. Sensor location bias sigma (δ), as defined by Chen *et al* (2011) as the normalised difference between the footprint-weighted spatial index, and the mean value of that index over the area of interest, in this case the 0.36 km² domain around the tower.

% δ	Elevation	Sedge	NDVI	NDWI
BES	−18	18	−26	51
BEO	−21	−32	−25	24

consisted mostly of the ‘zero curtain’ period, when soil remains unfrozen around zero degrees, was characterised by stable and substantial CH₄ emissions rates, though lower than those during summer (Zona *et al* 2016).

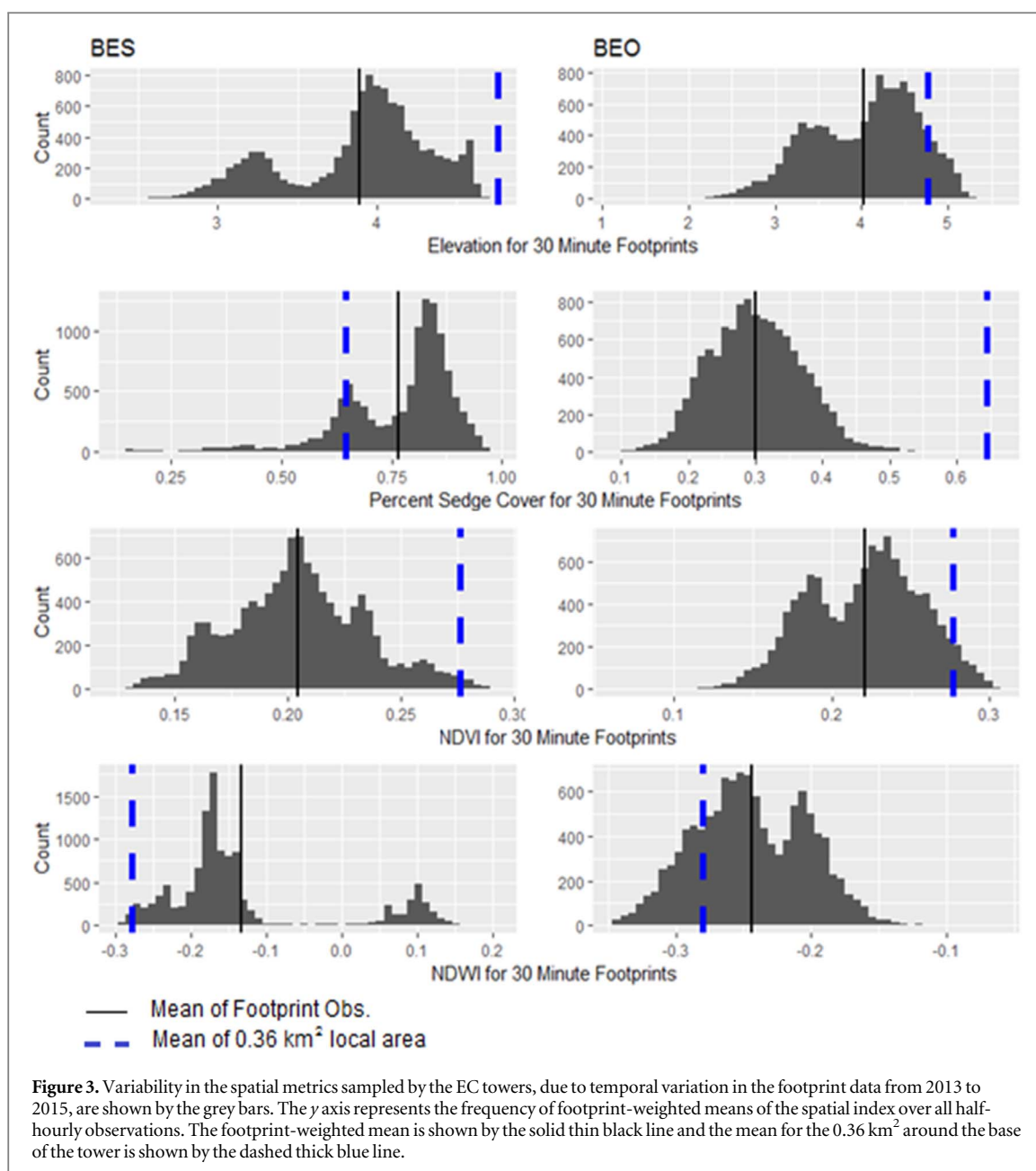
3. Results

3.1. Spatial variability and sensor location bias

The footprint modelling showed that there was substantial variability in the footprint-weighted spatial indices (figure 3). The means of the footprint-weighted spatial indices deviated substantially from the means for the 0.36 km² domain; the magnitude of the sensor location bias sigma, δ , varied among sites and the indices considered, ranging from |18|% to |51|% (table 1, figure 3). BES was more inundated than BEO, with generally higher sedge cover. BES presented a more defined bi-modal distribution of the spatial variables (figure 3), consistent with two very different ecosystem types measured: a drained lake basin (where the EC tower was located), surrounded by polygonised upland tundra. A wet meadow prevails east of the EC tower within the drained lake basin and is characterised by a lower elevation and higher sedge cover. A drier ecosystem prevails west of the tower, with a higher elevation and lower sedge cover (figure 2). The δ was between |18|% and |32|% for nearly all the spatial variables, except for $\widehat{\text{NDWI}}$ at BES, which showed a δ of more than |50|% (table 1). The lowest δ was in the sedge cover and elevation in BES (table 1).

3.2. Temporal and spatial controls on CH₄ fluxes

Using a linear model, we could explain 60% of the CH₄ flux variability for the full methane flux dataset (table 2). This model retained the temporal variables, soil temperature (T_S), SWC, and PAR, as well as, the spatial indexes, $\widehat{\text{NDVI}}$ and $\widehat{\text{NDWI}}$. The model including only spatial variables, was able to explain 33% of the variability in CH₄ emissions; when the model was limited to temporal variables, 53% of the variability in CH₄ emissions was explained, with soil temperature (T_S) having the largest explanatory power (51%) (table 2). In the residual analysis and when the temporal variation in the CH₄ fluxes was accounted for, the footprint-weighted spatial indices were able to explain 7% of the remaining variability in CH₄ fluxes.



In all periods, the single temporal variable with the most explanatory power was soil temperature (T_s), except for the snow melt period at BEO, where NDVI_{MODIS} performed better. Generally, when sites and seasons were modelled separately, the explanatory power of the spatial indices doubled for most time periods to ~20% (table 2). During the curtain period at BES the spatial indexes seemed to have little relevance (table 2). There was, however, little consistency in terms of which spatial index had explanatory power and they often only achieved moderate explanatory power even when used together.

4. Discussion

The results of this study support the importance of footprint modelling in heterogeneous environments,

as found in earlier studies (Budishchev *et al* 2014, Tuovinen *et al* 2018). In previous work, Wang *et al* (2016) used a threshold for δ of 10%, i.e. $|\delta| < 10$, when evaluating flux towers in the Canadian flux network, to determine if tower data would be suitable for upscaling fluxes to the regional scale. The lowest observed value of δ in this study was 18% spatial bias and in the case of NDWI, one of the spatial metrics that helped explain methane flux, had a bias of 51% (table 1). In another recent study, Treat *et al* (2018) found a 20%–65% underestimation of CH₄ emissions flux from a Siberian wetland site unless a high resolution wetland classification was used. While Tuovinen *et al* (2018), observed a somewhat contrasting result, in a Siberian shrub tundra site, where despite seeing a significant spatial bias (14%) and formally showing a 13% overestimation of methane flux for a 35.8 km² area, the results were not

Table 2. Results from linear modelling. The ‘Explanatory Variables’ column indicates which variables were included as follows: temporal: air temperature (T_A), soil temperature (T_S), soil water content (SWC), photosynthetically active radiation (PAR), atmospheric stability (Zol), friction velocity (u^*), air pressure (P_A), NDVI from the MODIS satellite ($NDVI_{MODIS}$), Spatial: \widehat{Elev} , \widehat{NDVI} , \widehat{NDWI} , \widehat{Sedge} (half-hourly footprint weighted means), remotely sensed (RS): $NDVI_{MODIS}$. Y is the dependent variable being modelled, either CH_4 emissions or the residuals from the temporal models (R_T) and the next two columns show the selected explanatory variables and the resulting adjusted r^2 value, for the indicated site, and season. All regressions shown are significant with p -values < 0.05 .

Site	Season	Explanatory variables	Y	Model	Adj. r^2
Both	All	All	CH_4	$\widehat{NDVI} + \widehat{NDWI} + T_S + SWC + PAR$	0.60
		Temporal	CH_4	$T_S + SWC + PAR$	0.53
		Temporal	CH_4	T_S	0.51
		Spatial	CH_4	$\widehat{Elev} + \widehat{Sedge}$	0.33
		RS	CH_4	$NDVI_{MODIS}$	0.35
		Spatial	R_T	$\widehat{Elev} + \widehat{NDVI} + \widehat{NDWI} + \widehat{Sedge}$	0.07
BES	Melt	Temporal	CH_4	T_S	0.20
		Spatial	R_T	\widehat{Sedge}	0.10
	Growing	Temporal	CH_4	T_S	0.20
		Spatial	R_T	$\widehat{NDWI} + \widehat{Sedge}$	0.15
	Curtain	Temporal	CH_4	T_S	0.27
		Spatial	R_T	$\widehat{Elev} + \widehat{NDVI} + \widehat{NDWI} + \widehat{Sedge}$	0.03
BEO	Melt	Temporal	CH_4	$NDVI_{MODIS}$	0.27
		Spatial	R_T	$\widehat{NDVI} + \widehat{NDWI}$	0.20
	Growing	Temporal	CH_4	T_S	0.30
		Spatial	R_T	$\widehat{Elev} + \widehat{NDVI} + \widehat{NDWI}$	0.22
	Curtain	Temporal	CH_4	T_S	0.38
		Spatial	R_T	\widehat{Sedge}	0.17

statistically significant. However, in this study they attributed fluxes to specific land cover classes and upscaled by using a single methane emission value for each class, that were calculated bases on measurements taken over one growing season. They acknowledged their results are heavily dependent on the landcover maps used and it could be a coincidence that the tower footprint was similar to the area to their area of interest. Additionally, they still concluded that in these heterogeneous sites, detailed footprint analysis is necessary, as they observed significant variability within their shrub tundra site. Our results suggest a similar over or underestimation of the CH_4 emissions could be generated if coarse-resolution data is used to upscale the EC data without accounting for footprint variability.

Our results indicate that variability in measured CH_4 flux can partially be attributed to changing footprint areas, in line with previous studies (Sachs *et al* 2010, Tagesson *et al* 2013). Overall, when site and season were accounted for, the explanatory power of the spatial indexes varied between 3% and 33% (table 2). During each season, different spatial metrics were better flux predictors for each of the sites. This highlights how polygonal tundra and the drained thermokarst are somewhat distinct habitats. In terms of seasonal variability, during the curtain period at BES the spatial indexes had relatively lower explanatory power, perhaps due to this area freezing up more uniformly. No one spatial index proved to be the most reliable CH_4 flux predictor, as the best results are often achieved when multiple indexes are used concurrently. Even the best spatial model left at least 40% of the variability in

CH_4 fluxes unexplained. This could be linked to the complex influence of these variables on CH_4 release not necessarily being captured by the simple models used in this study (Sebacher *et al* 1983, Herbst *et al* 2011, Matthes *et al* 2014). For example, Göckede *et al* (2019) found that 3%–4% of methane emissions in their wetland study site in the Russian Arctic were in the form of sporadic bursts; a linear model might not be ideal to capture this type of emission pattern. Furthermore, the snow melt season it is a period of rapid transition, where NDVI and NDWI would vary greatly. Subsequent research might significantly improve the explanatory power of the spatial indices by utilising drones to collect high-resolution time series of these metrics. With appropriate development, these results could further develop upscaling methods and improve the extrapolation of the site-level data to the regional scale.

5. Conclusions

The overarching result from this study is to highlight the necessity of high-resolution footprint modelling when interpreting EC data from heterogeneous environments. One cannot assume that the tower footprint is representative of the even the immediate domain around the tower. Our analysis also shows that the area sampled by the towers differs from the surrounding local domain by |18|% to |51|%, depending on the spatial index used. The results of this study also show that spatial variability in the EC tower footprint in these Arctic wetlands sites accounts for a significant

amount of the half-hourly variance in the measured CH₄ flux. Models derived using high-resolution data should not be directly applied to lower resolution RS data, such as MODIS data, unless one accounts for footprint variability. The explanatory power of the spatial metrics varies, between 3% and 33%, depending on the site, time period and the modelling approach. Recognising this potential source of error is particularly valuable given that EC data are used to estimate regional and global CH₄ budgets.

To test the larger scale applicability of the results, this analysis should be expanded to include data from additional years and a variety of tundra sites across the Arctic. One might also evaluate whether using different footprint models, such as Vesala *et al* (2008) or Kljun *et al* (2004), would help refine the footprint analysis. These steps would help develop an improved methodology for upscaling CH₄ fluxes in the Arctic.

Acknowledgments

This project was funded through the National Science Foundation (NSF) Office of Polar Programs via a grant to D Zona and W C Oechel (award number 1204263, and 1702797) and by the ABoVE (NNX15AT74A; NNX16AF94A) grants awarded to W C Oechel and D Zona. This research was conducted on land owned by the Ukpavik Inupiat Corporation (UIC). This project has received funding from the European Union's Horizon 2020 research and innovation program under grant agreement No. 727890, the NERC UAMS Grant (NE/P002552/1) to D Zona and W C Oechel, and the NERC ACCE DTP PhD (NE/L002450/1) grant awarded to K Reuss-Schmidt. The collection of the LiDAR DEM was supported by the Department of Energy, Office of Science, Biological and Environmental Research program, Next Generation Ecosystem Experiment, DOE NGEE-Arctic project. We would like to thank the Global Change Research Group at San Diego State University for the help in the field, and UMIAQ and UIC for logistical support. We would like to thank the team at the Polar Geospatial Centre under NSF OPP awards 1043681 and 1559691 for providing the satellite imagery. We also would like to thank Douglas Stow and Trent Biggs for the suggestions on the remote sensing and hydrological model analyses.

Data availability statement

The eddy covariance data (<http://doi.org/10.18739/A2TM72117>) and LiDAR digital elevation (<http://doi.org/10.5440/1224720>) model utilized in this study are freely available for use. The landcover classification and footprint modelling data may be made available upon reasonable request to Craig Tweedie (please use form on <http://barrowmapped.org>), and Cassandra Reuss-Schmidt (kreuss-schmidt1@sheffield.ac.uk) respectively.

Finally, the Worldview 2 data may be purchased from DigitalGlobe.

ORCID iDs

Kassandra Reuss-Schmidt  <https://orcid.org/0000-0002-8382-5547>

References

- Andresen C G, Lara M J, Tweedie C E and Lougheed V L 2017 Rising plant-mediated methane emissions from arctic wetlands *Glob. Change Biol.* **23** 1128–39
- Baldocchi D D 2003 Assessing the eddy covariance technique for evaluating carbon dioxide exchange rates of ecosystems: past, present and future *Glob. Change Biol.* **9** 479–92
- Blunden J and Arndt D S 2019 State of the Climate in 2018 *Bull. Am. Meteorol. Soc.* **100** S305
- Brown J 1967 Tundra soils formed over ice wedges, northern Alaska *Soil Sci. Soc. Am. J.* **31** 686–91
- Budishchev A, Mi Y, Van Huissteden J, Beileli-Marchesini L, Schaepman-Strub G, Parmentier F, Fratini G, Gallagher A, Maximov T and Dolman A 2014 Evaluation of a plot scale methane emission model at the ecosystem scale using eddy covariance observations and footprint modelling *Biogeosciences Discuss.* **11** 3927–61
- Burba G and Anderson D 2010 *A Brief Practical Guide to Eddy Covariance Flux Measurements: Principles and Workflow Examples for Scientific and Industrial Applications* (Lincoln, NE: LI-COR)
- Chen B, Black T A, Coops N C, Hilker T, Trofymow J T and Morgenstern K 2009 Assessing tower flux footprint climatology and scaling between remotely sensed and eddy covariance measurements *Bound. Layer Meteorol.* **130** 137–67
- Chen B, Coops N C, Fu D, Margolis H A, Amiro B D, Barr A G, Black T A, Arain M A, Bourque C P-A and Flanagan L B 2011 Assessing eddy-covariance flux tower location bias across the Fluxnet-Canada research network based on remote sensing and footprint modelling *Agric. For. Meteorol.* **151** 87–100
- Davidson S J, Santos M J, Sloan V L, Reuss-Schmidt K, Phoenix G K, Oechel W C and Zona D 2017 Upscaling CH₄ fluxes using high-resolution imagery in arctic tundra ecosystems *Remote Sens.* **9** 1227
- Davidson S J, Sloan V L, Phoenix G K, Wagner R, Fisher J P, Oechel W C and Zona D 2016 Vegetation type dominates the spatial variability in CH₄ emissions across multiple arctic tundra landscapes *Ecosystems* **19** 1–17
- Didan K 2015 *MOD13Q1 MODIS/Terra Vegetation Indices 16-Day L3 Global 250m SIN Grid V006 [Data set]* NASA EOSDIS Land Processes DAAC (<https://doi.org/10.5067/MODIS/MOD13Q1.006>) (Accessed: 22 November 2019)
- Etminan M, Myhre G, Highwood E and Shine K 2016 Radiative forcing of carbon dioxide, methane, and nitrous oxide: a significant revision of the methane radiative forcing *Geophys. Res. Lett.* **43** 12,614–23
- Foken T, Göckede M, Mauder M, Mahrt L, Amiro B and Munger W 2004 Post-field data quality control *Handbook of Micrometeorology* (Berlin: Springer)
- Foken T and Wichura B 1996 Tools for quality assessment of surface-based flux measurements *Agric. For. Meteorol.* **78** 83–105
- Forster P, Ramaswamy V, Artaxo P, Bernsten T, Betts R, Fahey D W, Haywood J, Lean J, Lowe D C and Myhre G 2007 Changes in atmospheric constituents and in radiative forcing *Climate Change 2007. The Physical Science Basis* Ch 2
- Gao B-C 1996 NDWI—a normalized difference water index for remote sensing of vegetation liquid water from space *Remote Sens. Environ.* **58** 257–66
- Göckede M, Kittler F and Schaller C 2019 Quantifying the impact of emission outbursts and non-stationary flow on eddy covariance CH₄ flux measurements using wavelet techniques *Biogeosciences Discuss.* **16** 3113–31

- Göckede M, Markkanen T, Hasager C B and Foken T 2006 Update of a footprint-based approach for the characterisation of complex measurement sites *Bound. Layer Meteorol.* **118** 635–55
- Goodrich J, Oechel W, Gioli B, Moreaux V, Murphy P, Burba G and Zona D 2016 Impact of different eddy covariance sensors, site set-up, and maintenance on the annual balance of CO₂ and CH₄ in the harsh Arctic environment *Agric. For. Meteorol.* **228** 239–51
- Hartley I, Hill T, Wade T, Clement R, Moncrieff J, Prieto-Blanco A, Disney M, Huntley B, Williams M and Howden N 2015 Quantifying landscape-level methane fluxes in subarctic Finland using a multiscale approach *Glob. Change Biol.* **21** 3712–25
- Herbst M, Friborg T, Ringgaard R and Soegaard H 2011 Interpreting the variations in atmospheric methane fluxes observed above a restored wetland *Agric. For. Meteorol.* **151** 841–53
- Horst T and Weil J 1994 How far is far enough?: the fetch requirements for micrometeorological measurement of surface fluxes *J. Atmos. Ocean. Technol.* **11** 1018–25
- Hsieh C-I, Katul G and Chi T-W 2000 An approximate analytical model for footprint estimation of scalar fluxes in thermally stratified atmospheric flows *Adv. Water Res.* **23** 765–72
- Hugelius G, Strauss J, Zubrzycki S, Harden J W, Schuur E, Ping C-L, Schirmermeister L, Grosse G, Michaelson G J and Koven C D 2014 Estimated stocks of circumpolar permafrost carbon with quantified uncertainty ranges and identified data gaps *Biogeosciences* **11** 6573–93
- IPCC 2013 The physical science basis *Contribution of Working Group I to the Fifth Assessment Report of The Intergovernmental Panel On Climate Change*. ed K Tignor *et al* p 1535
- Joabsson A, Christensen T R and Wallén B 1999 Influence of vascular plant photosynthetic rate on CH₄ emission from peat monoliths from southern boreal Sweden *Polar Res.* **18** 215–20
- Kljun N, Calanca P, Rotach M and Schmid H 2004 A simple parameterisation for flux footprint predictions *Bound. Layer Meteorol.* **112** 503–23
- Kormann R and Meixner F X 2001 An analytical footprint model for non-neutral stratification *Bound. Layer Meteorol.* **99** 207–24
- Lara M J, Mcguire A D, Euskirchen E S, Tweedie C E, Hinkel K M, Skurikhin A N, Romanovsky V E, Grosse G, Bolton W R and Genet H 2015 Polygonal tundra geomorphological change in response to warming alters future CO₂ and CH₄ flux on the Barrow Peninsula *Glob. Change Biol.* **21** 1634–51
- Leclerc M and Thurtell G 1990 Footprint prediction of scalar fluxes using a Markovian analysis *Bound. Layer Meteorol.* **52** 247–58
- Leclerc M Y and Foken T 2014 *Footprints in Micrometeorology and Ecology* (Berlin: Springer)
- Lipson D A, Zona D, Raab T K, Bozzolo F, Mauritz M and Oechel W C 2012 Water table height and microtopography control Biogeochemical cycling in an Arctic coastal tundra ecosystem *Biogeosciences* **9** 577–91
- Matthes J H, Sturtevant C, Verfaillie J, Knox S and Baldocchi D 2014 Parsing the variability in CH₄ flux at a spatially heterogeneous wetland: Integrating multiple eddy covariance towers with high-resolution flux footprint analysis *J. Geophys. Res.: Biogeosciences* **119** 1322–39
- Mcewing K R, Fisher J P and Zona D 2015 Environmental and vegetation controls on the spatial variability of CH₄ emission from wet-sedge and tussock tundra ecosystems in the Arctic *Plant Soil* **388** 37–52
- Parmentier F, Van Huissteden J, Van Der Molen M, Schaepman-Strub G, Karsanaev S, Maximov T and Dolman A 2011 Spatial and temporal dynamics in eddy covariance observations of methane fluxes at a tundra site in northeastern Siberia *J. Geophys. Res.: Biogeosciences* **116** G03016
- Sachs T, Giebels M, Boike J and Kutzbach L 2010 Environmental controls on CH₄ emission from polygonal tundra on the microsite scale in the Lena river delta, Siberia *Glob. Change Biol.* **16** 3096–110
- Schmid H P and Lloyd C R 1999 Spatial representativeness and the location bias of flux footprints over inhomogeneous areas *Agric. For. Meteorol.* **93** 195–209
- Schuepp P, Leclerc M, Macpherson J and Desjardins R 1990 Footprint prediction of scalar fluxes from analytical solutions of the diffusion equation *Bound. Layer Meteorol.* **50** 355–73
- Schuur E, Abbott B, Bowden W, Brovkin V, Camill P, Canadell J, Chanton J, Chapin Iii F, Christensen T and Ciais P 2013 Expert assessment of vulnerability of permafrost carbon to climate change *Clim. Change* **119** 359–74
- Schuur E A and Abbott B 2011 Climate change: high risk of permafrost thaw *Nature* **480** 32–3
- Sebacher D I, Harriss R C and Bartlett K B 1983 Methane flux across the air-water interface: air velocity effects *Tellus B* **35** 103–9
- Segers R 1998 Methane production and methane consumption: a review of processes underlying wetland methane fluxes *Biogeochemistry* **41** 23–51
- Sturtevant C S and Oechel W C 2013 Spatial variation in landscape-level CO₂ and CH₄ fluxes from arctic coastal tundra: influence from vegetation, wetness, and the thaw lake cycle *Glob. Change Biol.* **19** 2853–66
- Tagesson T, Mastepanov M, Mölder M, Tamstorf M P, Eklundh L, Smith B, Sigsgaard C, Lund M, Ekberg A and Falk J M 2013 Modelling of growing season methane fluxes in a high-Arctic wet tundra ecosystem 1997–2010 using *in situ* and high-resolution satellite data *Tellus B* **65** 19722
- Taş N, Prestat E, Wang S, Wu Y, Ulrich C, Kneafsey T, Tringe S G, Torn M S, Hubbard S S and Jansson J K 2018 Landscape topography structures the soil microbiome in arctic polygonal tundra *Nat. Commun.* **9** 777
- Treat C C, Bloom A A and Marushchak M E 2018 Nongrowing season methane emissions—a significant component of annual emissions across northern ecosystems *Glob. Change Biol.* **24** 3331–43
- Tuovinen J-P, Aurela M, Hatakka J, Räsänen A, Virtanen T, Mikola J, Ivakhov V, Kondratyev V and Laurila T 2018 Interpreting eddy covariance data from heterogeneous Siberian tundra: land cover-specific methane fluxes and spatial representativeness *Biogeosciences* **16** 255–74
- Valentine D W, Holland E A and Schimel D S 1994 Ecosystem and physiological controls over methane production in northern wetlands *J. Geophys. Res.: Atmos.* **99** 1563–71
- Vaughn L J, Conrad M E, Bill M and Torn M S 2016 Isotopic insights into methane production, oxidation, and emissions in Arctic polygon tundra *Glob. Change Biol.* **22** 3487–502
- Vesala T, Kljun N, Rannik Ü, Rinne J, Sogachev A, Markkanen T, Sabelfeld K, Foken T and Leclerc M 2008 Flux and concentration footprint modelling: state of the art *Environ. Pollut.* **152** 653–66
- Von Fischer J C, Rhew R C, Ames G M, Fosdick B K and Von Fischer P E 2010 Vegetation height and other controls of spatial variability in methane emissions from the Arctic coastal tundra at Barrow, Alaska *J. Geophys. Res.: Biogeosciences* **115** G00103
- Wang H, Jia G, Zhang A and Miao C 2016 Assessment of spatial representativeness of eddy covariance flux data from flux tower to regional grid *Remote Sens.* **8** 742
- Wilson C and Altmann G 2015 *Digital Elevation Model, 0.25 m, Barrow Environmental Observatory, Alaska, 2013., Next-Generation Ecosystem Experiments (NGEE) Arctic Project* (Oak Ridge National Laboratory) (<https://doi.org/10.5440/1224720>)
- Zheng J, Roychowdhury T, Yang Z, Gu B, Wulschleger S D and Graham D E 2018 Impacts of temperature and soil characteristics on methane production and oxidation in Arctic tundra *Biogeosciences* **15** 6621–35
- Zona D 2019 *Greenhouse Gas Flux Measurements at the Zero Curtain North Slope, Alaska, 2012–2017. Arctic Data Center* (<https://doi.org/10.18739/A2TM72117>)
- Zona D, Gioli B, Commane R, Lindsaas J, Wofsy S C, Miller C E, Dinardo S J, Dengel S, Sweeney C and Karion A 2016 Cold season emissions dominate the Arctic tundra methane budget *Proc. Natl Acad. Sci.* **113** 40–5
- Zona D, Oechel W, Kochendorfer J, Paw U, Salyuk A, Olivas P, Oberbauer S and Lipson D 2009 Methane fluxes during the initiation of a large-scale water table manipulation experiment in the Alaskan Arctic tundra *Glob. Biogeochem. Cycles* **23**